Multimed Tools Appl (2017) 76:5787–5802
DOI 10.1007/s11042-014-2408-1

Distribution of primary additional errors in fractal encoding method

Shuai Liu · Weina Fu · Liqiang He · Jiantao Zhou · Ming Ma

Received: 30 October 2014 / Revised: 19 November 2014 / Accepted: 27 November 2014 /
Published online: 6 December 2014

Abstract Today, fractal image encoding method becomes an effective loss compression method in multimedia without resolution, and its negativeness is that its high computational complexity. So many approximate methods are given to decrease the computation time. So the distribution of error points is valued to research. In this paper, by extracted primary additional error values, we first present a novel fast fractal encoding method. Then, with the extracted primary additional error values, we abstract the distribution of these values. We find that the different distribution of values denotes the different parts in images. Finally, we analyze the experimental results and find some properties of these values. The experimental results also show the effectiveness of the method.

Keywords Image enoding · Fractal encoding · Primary additional error · Distribution · Edge

1 Introduction

With the rapid improvement of computer science and network, multimedia becomes an important research area today. Multimedia contains more information than words,

S. Liu · W. Fu · L. He · J. Zhou · M. Ma
College of Computer Science, Inner Mongolia University, Hohhot 010012, China

S. Liu
e-mail: Cs_liushuai@imu.edu.cn

W. Fu
e-mail: Wn_fu@sohu.com

J. Zhou
e-mail: cszjtao@imu.edu.cn

M. Ma
e-mail: csmaming@imu.edu.cn

S. Liu
School of Physical Science and Technology, Inner Mongolia University, Hohhot 010012, China

L. He (✉)
Room A311, Computer Building, Inner Mongolia University, No. 235, Western University Street, Hohhot 010012, China
e-mail: liqiang@imu.edu.cn

but the negativeness of its application is the large size. Nowadays, the increment of multimedia size needs huge space to store and large bandwidth to transfer. So decrease of the multimedia is a highlight in research. Furthermore, decrease of image, which is the basis in this area, also shows its importance.

Today, based on the improvement of multimedia, many classic image encoding methods and international standard of multimedia have been presented. For example, discrete cosine transform (DCT) [24], Huffman code [9], wavelet image coding [25], etc. are all multimedia classic encoding methods. Meanwhile, BIG, JPEG, H.263, MPEG, etc. are all international standards.

But in nature, the geometrical form is usually not regular and smooth. In fact, artificial objects usually have the regular and smooth form, which can be processed by traditional geometry. However, nature objects are usually rough and anomalistic. In this way, since 1980s, a novel subject is created to research in the non-classical geometry. It is called fractal geometry [6, 21].

The basic thinking of fractal is to reach the scale of self-similarity of the whole and the part because most nature objects have the properties of self-similarity, just like in galaxies, lasers and waves [8, 10, 23].

Then, with Banach Fixed Point Theorem as a theoretical support, researchers can use the contractive affine transformation (CAT) into the image encoding study [7, 26]. This is a novel thinking in the image encoding study. It is called fractal image encoding. In this method, it first finds the self-similarity in whole-part of images. Then it stores the quantization parameters of CAT as an encoding file. So the encoding file is much smaller than the original image. In this case, it can reach higher compressing ratio.

In fact, fractal image encoding method has many benefits. One benefit is that this method with same parameters reaches fixed compressing ration for all images with same size. Then, by the proof of existence and uniqueness of the iteration, the final mapping image will always reach the original image with any initial mapping image. In other words, the original image is the ultimate limit of the iteration.

But as the fractal encoding method is a finite distortion method, it loses some points' value indeed. Then, we believe that the lost values are not same for every image and there are some hidden relations between these values and the images.

So, in this paper, we present the distributions of images with different kinds by used the proposed primary additional errors. First, we exact additional primary errors, which are added to compensate the decoding image. In this case, the fast fractal coding method is proposed. Then, we analyze these errors and find a novel method to classify the images based on the distribution of primary additional errors.

The remainder of the paper is organized as follows. Related works are presented in Section 2. Then, we present the novel fractal encoding method with primary additional errors in Section 3. Furthermore, we study the distribution of images by the primary additional errors in Section 4. Finally, Section 5 summarizes the whole paper.

2 Related works

First, Barnsley and Jacquin used iterated function system (IFS) and Recurrent Iterated Function System (RIFS) in image encoding area [1]. They reached a highest compressing ratio more than 10000:1 for some special images. Then, Jacquin

developed a software system of self-adaptive fractal encoding method [11]. The generation of the system is soon studied and improved by many researchers. At the same time, Monro and Dudbridge also found the fractal block in images and presented their fractal encoding method [22]. Furthermore, Bedford et al. presented a fractal encoding method in monochrome images, and Kim and Park presented theirs in still image by fractal approximation [2, 13]. Kim et al. focused on the mapping and non-contractive interframe mapping in the video, and presented a fractal encoding method in video sequence [12]. Chang and Kuo designed a domain pool and presented an iteration-free fractal image encoding method based on the pool [5].

Since 2000s, based on the rapid increments of multimedia, especially the images, fractal image encoding also progressed quickly. The mainly study domains are two, which are (i) increase the encoding rate and (ii) decrease the encoding time. There are many methods are presented based on many thinking. Li et al. present a fractal encoding method by used fuzzy image metric [15]. Lai et al. presented a fast fractal image encoding method by used kick-out and zero contrast conditions [14]. Belloulata encoded subbands by used non-iterative block clustering [3]. Wang et al. found a modified gray level transform and fitting plane and presented a no-search fractal image encoding method [28, 29]. He also used wavelet transform into fractal encoding method [30, 32]. Lu et al. used fitting plane into Huber fractal encoding method [20]. Bhayani and Thanushkodi found some properties of medical image and used fractal encoding method into medical image compression [4]. Our team also reached some results in this area. We researched fractal properties in k-M set and use it into facial capture [16, 18].

As the fractal encoding method lost some points' value indeed, the lost values must have some hidden relations with the original images. So if we can reach the relation, we can classify or separate the images by used the relation. In this way, this paper encoded some images to find the distribution of these images.

3 Fractal encoding method by used primary additional errors

First, we present the steps of a fractal image encoding method in Fig. 1.

Then, we propose the improved fractal image encoding and decoding method in Alg. 1a and Alg. 1b, In which I means original image, n means the size of I is n×n, c means the size of sub-image is c×c in encoding set (c|n), d=n/c, f means the size of sub-image is f×f in affine set (f<c), F means the encoding file.

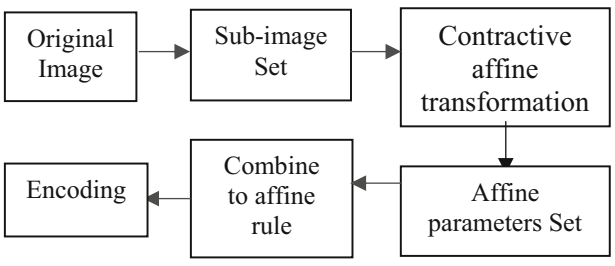

Fig. 1 Process of fractal image encoding method

Algorithm 1a. Fractal Encoding Method with Primary Additional Error

Input. I(n×n); c; f.

Output. F.

Step 1.

To find a partition I_r of I ($r=1,2,\ldots,d^2$), which means that $\forall$ i, j|$i\neq j\rightarrow I_i\cap I_j=\varnothing$ and $U_{1\le i\le d}I_i$=I is a tautology. Meanwhile, in this partition, $\forall$ i, j| scale of I_i=scale of I_j=cc is a tautology.

Step 2.

To divide I to part-repeatable D_k. The size of all D_k is f.

Step 3.

For every I_r do

To find the best affine transformation of I_r in D_k, and store it as a vector in the affine transformation table.

Step 4.

To extract primary additional errors and store them in the matrix of primary additional errors (PAE). Then, output the fusion of both affine transforming table and PAE as encoding file F.

Alg. 1a finished

In following, decoding method is presented in Alg.1b, in which s means the scaling of luminance, o means offset of luminance, (x, y) mean the starting position of affine transformation, direction means the eight types of equilong transformations, T means the iterating time, D means the decoding images. Others are same to Alg. 1a.

Algorithm 1b. Fractal Decoding Method with Primary Additional Error

Input. F.

Output. D.

Step 1.

To extract PAE and affine transforming table from F.

Step 2.

While the affine transforming table is not finished.

To extract a vector from affine transforming table, which in a best affine transformation of I_r in D_k. To locate the position by used (x, y). To iterate a blank sub-image with size f×f by used corresponding s and o. Then, to process equilong transformation by used direction.

Step 3.

To collage all rectangular areas to an image D′. Then, let R_i = corresponding part of D′, iterating step 1—3 until iterating time = T.

Step 4.

To output D′ as D.

Alg. 1b finished.

Here, we present six figures with same size 256×256 in Fig. 2 as the original images in our experiment, where Fig. 2a is classic “Lena”, Fig. 2b is classic “bird”, Fig. 2c is classic “baboon”, Fig. 2d is classic “Barbara”, Fig. 2e is classic “fractal”, Fig. 2f is classic “fruit”.

Then, we use Alg. 1a to encode these original figures and Alg. 1b to decode these encoding files to decoding images. The decoding results are presented in Fig. 3, where the left sub-figure

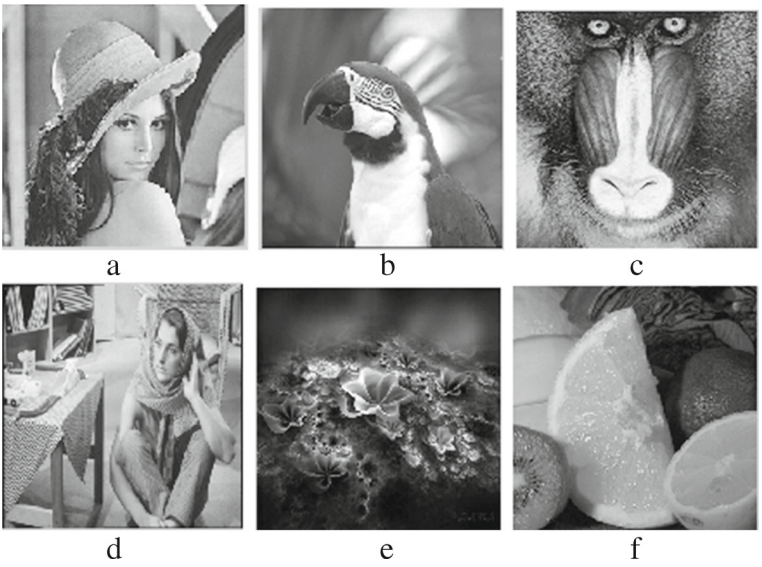

Fig. 2 Original images

in every row is decoding image with one iterating time, the middle is decoding image with three iterating times, and the right is decoding image with five iterating times.

Figure 4 presents the encoding files of these original images, in which the symbols are corresponding to Fig. 2. In Fig. 4, we find the encoding files are divided into two parts. The left part in every sub-figures of Fig. 4 is the encoding s, o and start position of iteration. The right part is the encoding PAE, directions and position of PAE.

Since we have extracted the PAE, we believe the quality of the decoding image is high enough. In fact, the PSNRs are computed to measure the quality of the decoding image from Eq. 1 and presented in Table 1 [27]. So we find the effectiveness of our method.

$$\mathrm{PSNR} = 10\cdot\log_{10}\frac{n^2\cdot 255^2}{\sum_{i=1}^{n^2}(I_i - D_i)^2} \tag{1}$$

4 Distribution of the primary additional error

Since the fractal image encoding is a finite distortion encoding method, there are error values in many image points. The errors between D and I appear because Eq. 3 is applied to instead of Eq. 2 in real application, in which B means the grey level, E means the identity matrix, $\|\ \|$ means the vector norm (usually 2-norm in fractal encoding), R_i means an affine sub- image, Dj means a pattern sub-image, m_i means serial number of the best D_j, s_i means scaling of R_i, o_i means offset of R_i in an affine mapping.

$$\frac{1}{B^2}\min_j\left\{\min_{s,o\in R,\ |s|<1}\left\|R_i - \left(s\cdot D_j + o\cdot E\right)\right\|^2\right\} \tag{2}$$

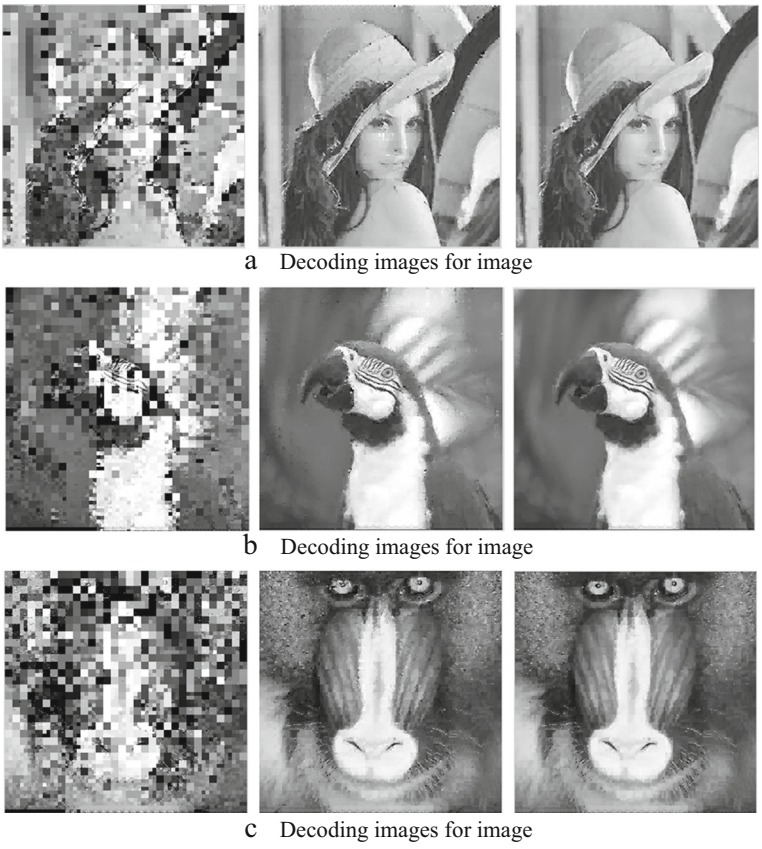

Fig. 3 Decoding images of Fig. 2 with 1 (*left*), 3 (*middle*) and 5 (*right*) iterating times

$$\min_{j}\left\{\min_{s,o\in R}\|R_i-\left(s\cdot D_j+o\cdot 1\right)\|\right\}=\min_{s,o\in R}\|R_i-\left(s_i\cdot D_{m_i}+o_i\cdot E\right)\| \quad (3)$$

These errors bring negativeness of visual effect in the decoding image. But we believe that not all of these errors bring the same scale of negativeness. In other words, there are several errors bring the mainly negativeness. So we extract PAE to find the properties of these errors.

In this way, we can extract additional error $\Delta_{n\times n}$ from Eq. 4, in which the symbols are same to Eqs. 2 and 3 where R_j^* denotes the decoding sub-images from D_j.

$$\Delta_{n\times n}=I_{n\times n}-\cup_{1\le j\le d}R_j^* \quad (4)$$

For all of the six original images, all Δs are computed and presented in Fig. 5 where c=8, f=4 (we also know n=256 from Fig. 2). The symbols of sub-figures are corresponding to Fig. 2. In Fig. 5, we know that the value zero in Δ of these images is usually not so much in general. But many values are small (no more than 50). So, in order to ensure the quality of visual effect for all images, we are more interesting in those points with high error values in Δ.

It is admittedly that blocking effect is an important element in visual effect for all images. So, those error values Δp and Δq of points p and q have to be stored when there is a common

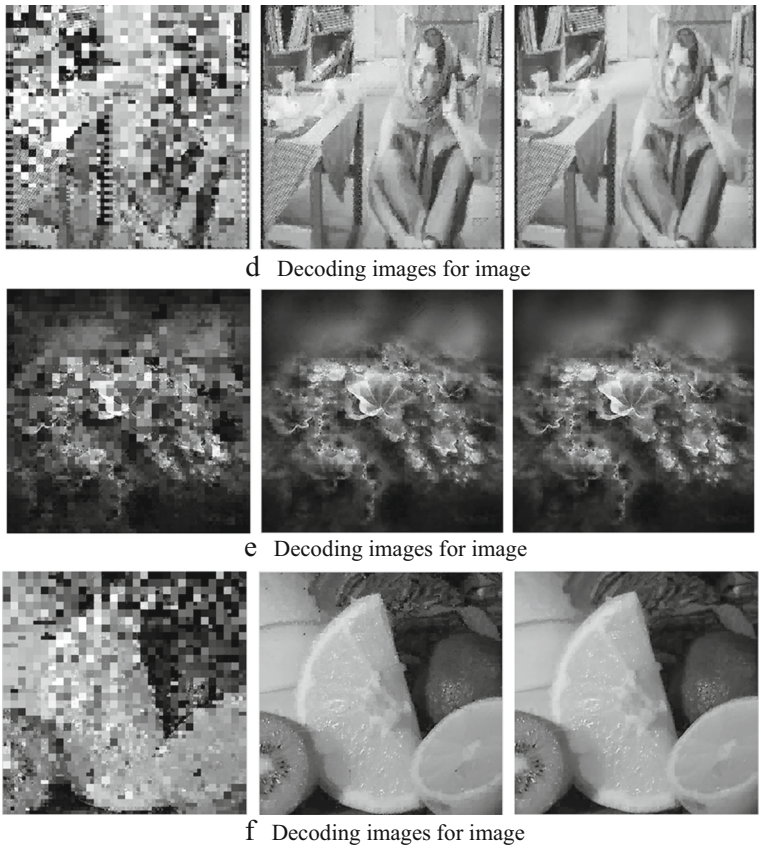

Fig. 3 (continued)

edge e of two image block D_p and D_q, $\Delta p \in D_p$, $\Delta q \in D_q$, and Δp, $\Delta q \in$ neighborhood of e. In this case, we have an evaluation standard to extract the valuable errors from Δ by the rule of Property 1 and present in Eq. 5 where $u_k=1+(1-k^{\ln 2})/e$ denotes the penalty weight of chromatic aberration between the error point and each other points within distance k where u_k is smaller when k is larger, (i, j) denotes the position of every error point, $(i', j') \in D_p$ when $(i, j) \in D_q$ and $(i', j') \in D_q$ when $(i, j) \in D_p$ denotes that $|i-i'|=t_1$ and $|j-j'|=t_2$ where $t_1+t_2=k$ and t_1, $t_2 N$. So Eq. 4 is the formation of PAE.

Property 1 The weights w_p and w_q of two random error points p and q conform to the following rule.

1) $w_p > w_q$ if $\Delta p > \Delta q$ with other elements equally.
2) $w_p \geq w_q$ if p is nearer to e than q with other elements equally.
3) $w_p > w_q$ if p has larger chromatic aberration around than q with other elements equally.

$$w_{i,j} = \Delta_{i,j} + \sum\nolimits_{k=1}^{m} u_k \cdot \frac{1}{k-1} \sum\nolimits_{i',j'} \left(\left| w_{i,j} - w_{i',j'} \right| \right) \tag{5}$$

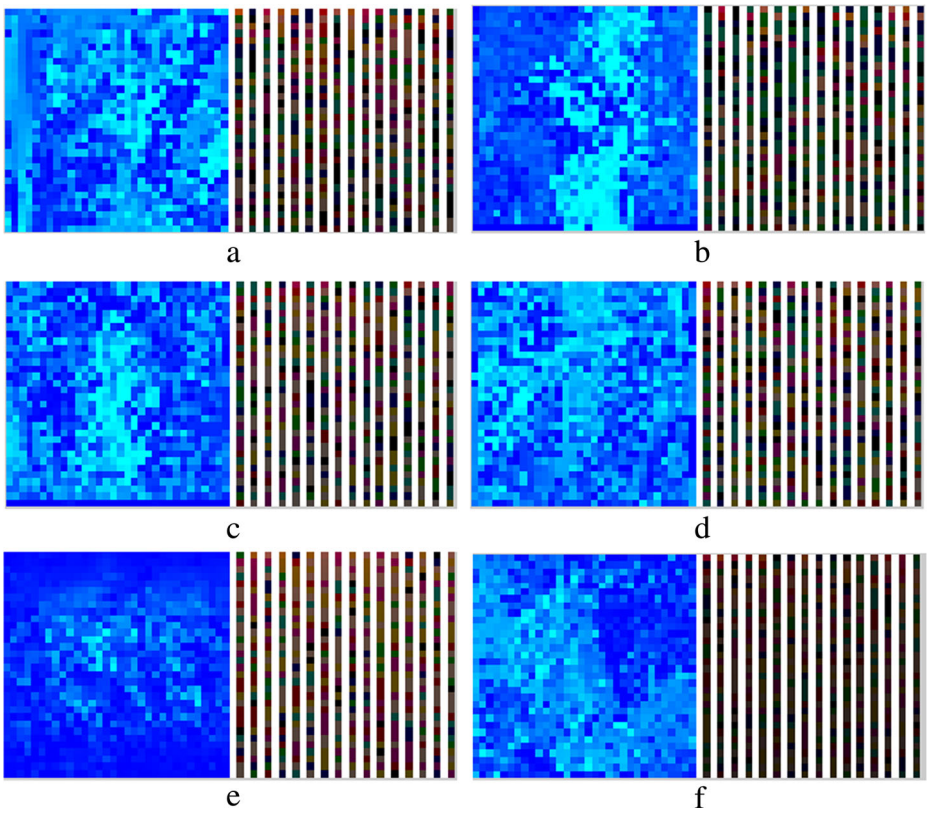

Fig. 4 Encoding files of the original images

Theorem 1 Eq. 5 conform to properties 1)-3) of Property 1.

Proof.

Assuming the two points p(i, j) and q(i^*, j^*), we have the following proof.

1) Case when $\Delta p > \Delta q$ with other elements equally.
We have $w_p - w_q = \Delta p - \Delta q > 0$ because $w_p - \Delta_p = wq - \Delta q$ (other elements equally). Case 1) is proved.

Table 1 Experimental results of fractal encoding method

Image	PSNR (dB)
Lena	26.49
Bird	30.59
Baboon	22.46
Barbara	22.95
fractal	25.50
fruit	30.67

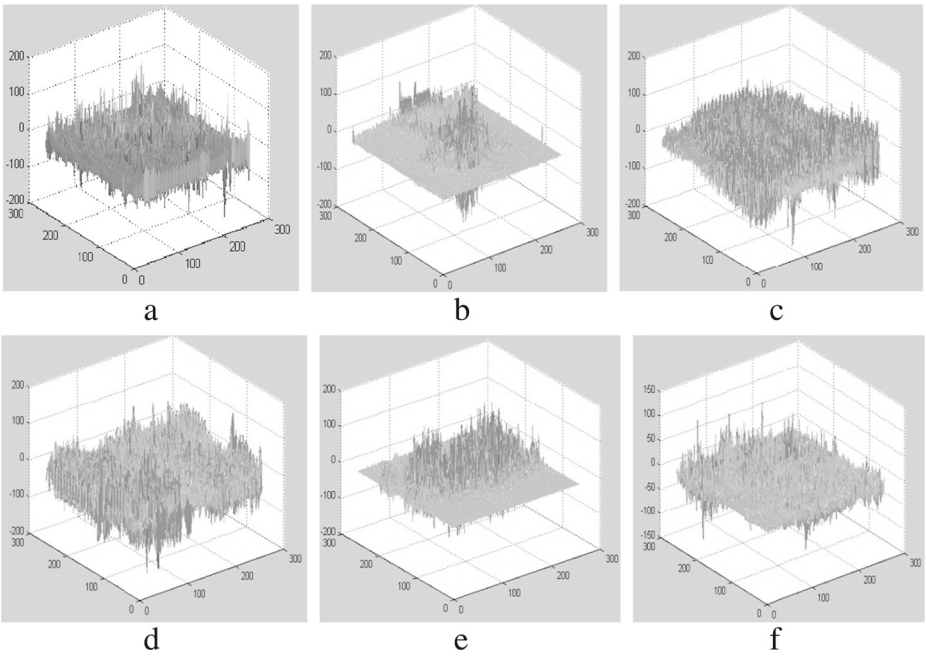

Fig. 5 Additional error values of the six original images

2) Case when p is nearer to e than q with other elements equally.

It is equivalent to that point p has at least one pixel nearer than point q and q is at least one pixel away from e. So, there is no point ($i^{*'}$, $j^{*'}$) makes k=1 around the point q. In this case, we have following Eq. 6 because $\Delta p=\Delta q$.

$$w_p - w_q = \sum_{k=1}^{m} u_k \cdot \frac{1}{k-1} \sum_{i',j'} \left(\left| w_{i,j} - w_{i',j'} \right| \right) - \sum_{k=2}^{m} u_k \cdot \frac{1}{k-1} \sum_{i^{*'},j^{*'}} \left(\left| w_{i*,j*} - w_{i^{*'},j*'} \right| \right) \quad (6)$$

Because of the other equal element of points p and q, we have following Eq. 7.

$$\sum_{k=1}^{m-1} u_k \cdot \frac{1}{k-1} \sum_{i',j'} \left(\left| w_{i,j} - w_{i',j'} \right| \right) = \sum_{k=2}^{m} u_{k-1} \cdot \frac{1}{k-1} \sum_{i^{*'},j^{*'}} \left(\left| w_{i*,j*} - w_{i^{*'},j*'} \right| \right) \quad (7)$$

So we have Eq. 8 to prove case 2) because $u_{k-1}>u_k$ and $u_m>0$. Case 2) is proved.

$$w_p - w_q = \sum_{k=2}^{m} (u_{k-1} - u_k) \cdot \frac{1}{k-1} \sum_{i',j'} \left(\left| w_{i,j} - w_{i',j'} \right| \right) + u_m \cdot \frac{1}{m-1} \sum_{i',j'} \left(\left| w_{i,j} - w_{i',j'} \right| \right) > 0 \quad (8)$$

3) Case when p has larger chromatic aberration around than q with other elements equally.

It means that $\sum_{i',j'} \left(\left| w_{i,j} - w_{i',j'} \right| \right) > \sum_{i^{*'},j^{*'}} \left(\left| w_{i*,j*} - w_{i^{*'},j*'} \right| \right)$. So we have Eq. 9 to prove case 3). Case 3) is proved.

$$w_p - w_q = \sum_{k=1}^{m} u_k \cdot \frac{1}{k-1} \left(\sum_{i',j'} \left(\left| w_{i,j} - w_{i',j'} \right| \right) - \sum_{i',j'} \left(\left| w_{i,j} - w_{i',j'} \right| \right) \right) > 0 \quad (9)$$

Then, theorem 1 is proved when cases 1)-3) are summarized.

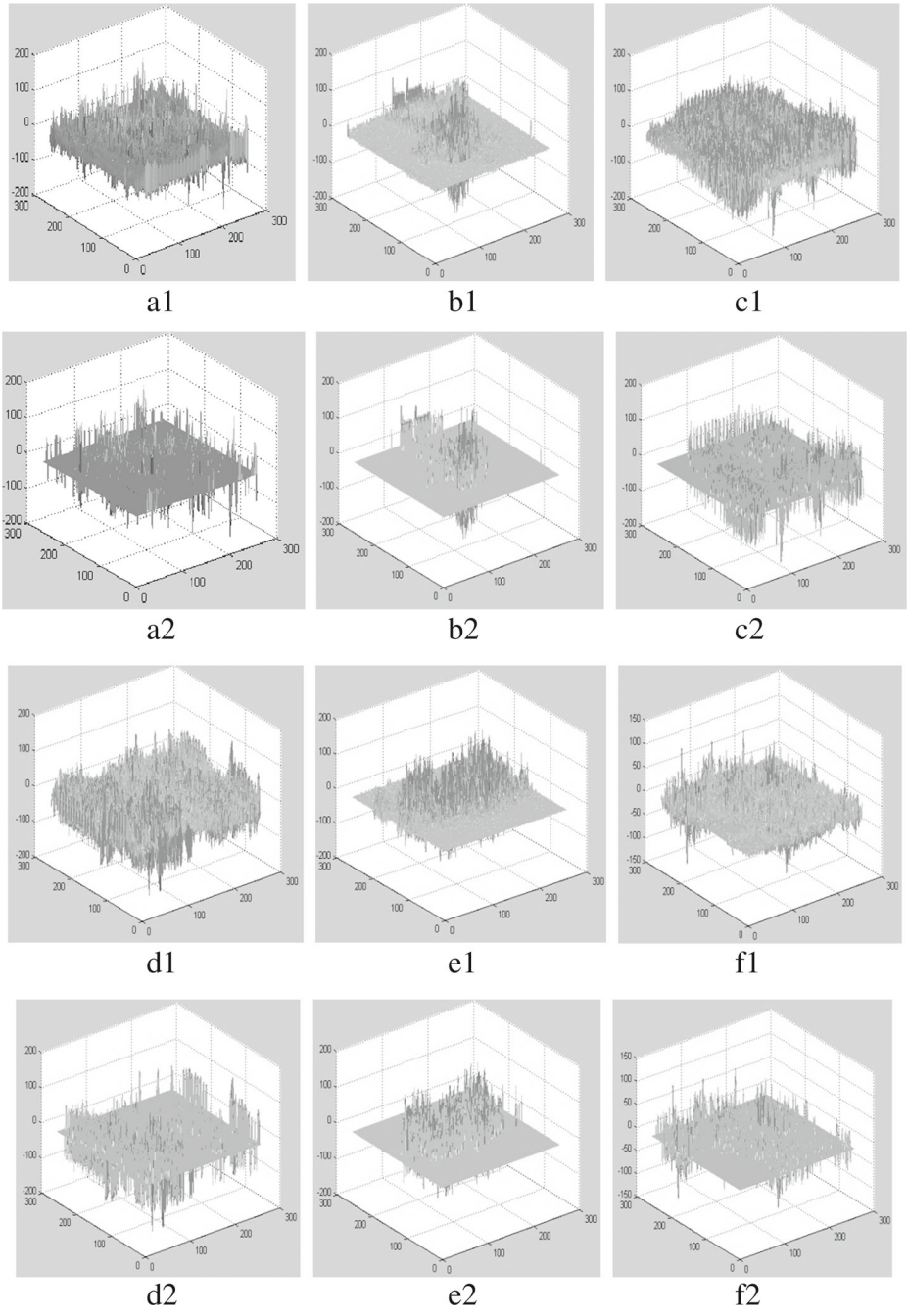

Fig. 6 Comparisons between total additional errors and PAE

In our experiment, we let m=5 because the blocking effect is small enough when m>5, and $u_k=1+(1-k^{\ln 2})/e$ because the blocking effect corresponds to the distance of the points

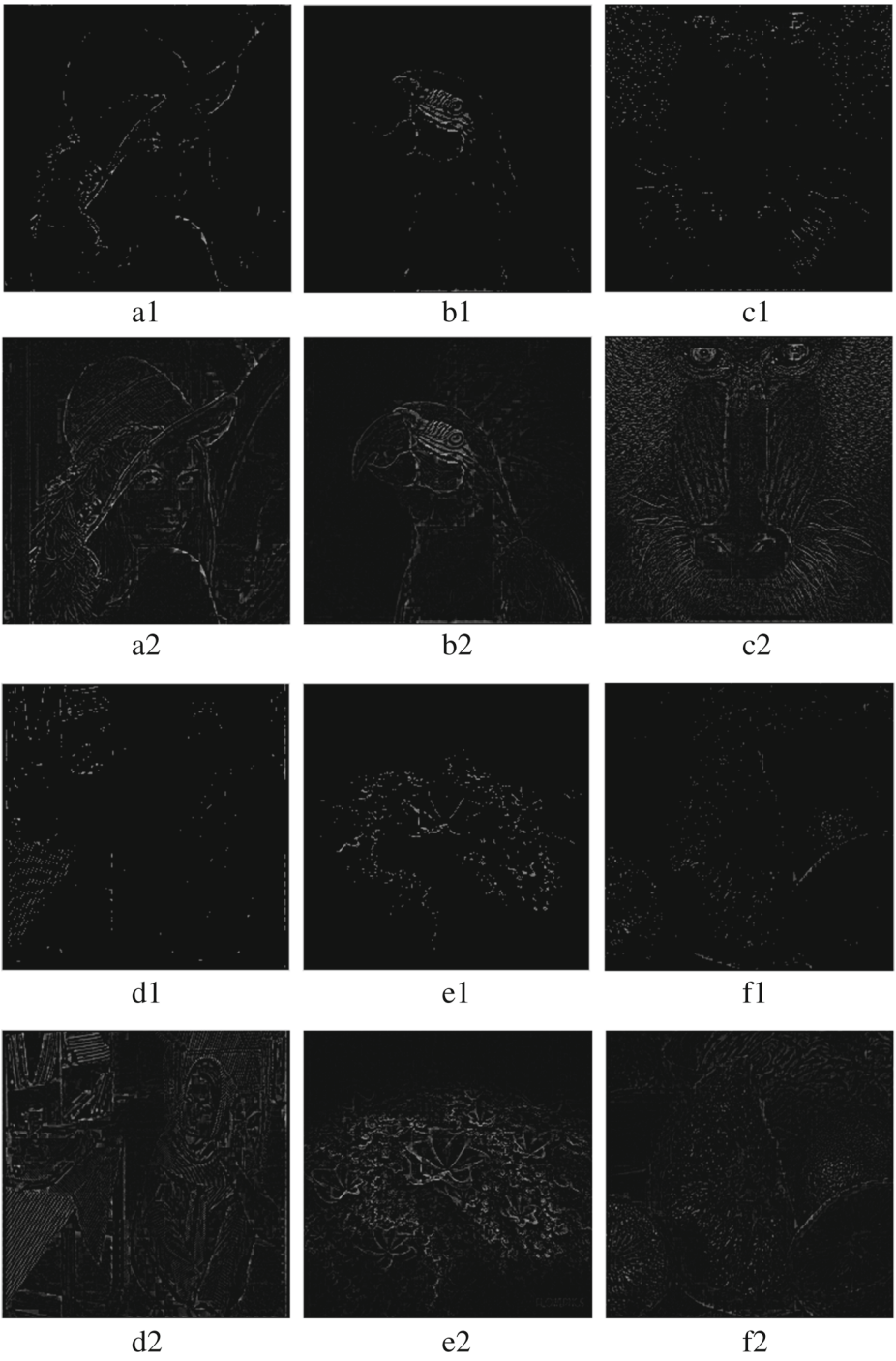

Fig. 7 Comparisons between visual PAE and extracted edges

(blocking effect is larger when the distance is smaller). Then, PAE are extracted by sequenced all w_{ij}. We extract PAE with d/2 points because they can be stored in the encoding file that they do not bring additional space cost. Furthermore, after we extract the PAE of these images, we can analyze their distributions.

With original images, we have both the additional error values and PAE of our method. They are presented in Fig. 6, where the sub-figures a1-e1 are additional errors of original images with the corresponding symbols and the sub-figures a2-f2 are additional errors without PAE of the corresponding original images.

First, we find some of the numerical characteristics in the additional errors. For example, the mean of value is 60~80 and maximum value is 150~200 in sub-figures a1-f1 of Fig. 6. Then, in sub-figures a2-f2, we find the additional errors change to 80~100 per point in PAE. It means that the formation we created to extract the PAE is effective. In other words, the PAE increase the encoding effect.

Then, in Fig. 6, the size of the matrix of addtional errors and PAE in sub-figures are same because the number of points is 256×256=65536. We present it in Fig. 6 by row major order. So in Fig. 6, we find that part of the PAE are around the edge of natural and artificial objects. The other part of PAE are around the inharmonious background. In other words, points of nature objects in the image mainly have small additional errors (see the small values in Figs. 6a1-6f1, they are all windows, hat, building, windwill, face, and other nature or harmonious objects et al.), and the points of inharmonious always have large additional errors (see the difference between Figs. 6a1-6f1 to Figs. 6a2-6f2, they are all factitious and inharmonious objects, the edge of person and window, tree and building, moving objects and background, et al.). So we know that we can divide the images to two parts, which are the natural (harmonious) background and inharmonious (artificial addition objects). Finally, the visual images of the PAE of all six images are shown in Fig. 7. We can find that the PAE are mostly distributed at edges of each images.

In Figs. a1-f1, we have the visual PAE and in Figs. a2-f2, we have the extracted edges. In this way, we find the most PAE come from the edges of each images.

5 Conclusion

In this paper, we present a distribution of primary additional errors. Experimental results shows that the primary additional errors distribute over the different objects in image and mostly around the across edge.

In this way, we know that the distribution of primary additional errors can be an effective classification of natural and artificial images. So in future, our work will pay attention to microcosmic encoding rule. We project to construct a rule of indemnity by used fuzzy set because of the classification of primary additional errors. Another area we want to study is to use parallel environment to increase coding time [17, 19, 31].

Acknowledgments This work is supported by Grants Postgraduate Scientific Research Innovation Foundation of Inner Mongolia [B20141012610Z], Programs of Higher-level talents of Inner Mongolia University [No. 125126, 115117, 135103], Scientific projects of higher school of Inner Mongolia [No. NJZY13004], Natural Science Foundation of Inner Mongolia [No. 2014BS0606, 2014BS0602], National Natural Science Foundation of China [No. 61261019, 61262082].

The authors wish to thank the anonymous reviewers for their helpful comments in reviewing this paper.

Conflict of interest The authors declare that there are no coflict of interest in this paper.

References

1. Barnsley MF, Jacquin AE (1988) Application of recurrent iterated function systems to images, in proceedings of the SPIE. Visual Commun Image Process 1001:122–131
2. Bedford T, Dekking FM, Breeuwer M et al (1994) Fractal coding of monochrome images [J]. Signal Process Image Commun 6(5):405–419
3. Belloulata K (2005) Fast fractal coding of subbands using a non-iterative block clustering [J]. J Vis Commun Image Represent 16(1):55–67
4. Bhavani S, Thanushkodi KG (2013) Comparison of fractal coding methods for medical image compression [J]. IET Image Process 7(7):686–693
5. Chang HT, Kuo CJ (2000) Iteration-free fractal image coding based on efficient domain pool design [J]. Image Process IEEE Trans 9(3):329–339
6. K Falconer (2003) Fractal geometry: mathematical foundations and applications, Second Edition [M]. John Wiley @ Sons, Inc
7. Goebel K, Kirk WA (1972) A fixed point theorem for asymptotically nonexpansive mappings [J]. Proc Am Math Soc 35(1):171–174
8. He JR, Yi L, Li HM (2014) Self-similar propagation and asymptotic optical waves in nonlinear waveguides [J]. Phys Rev E 90(1):013202
9. Huffman DA (1952) A method for the construction of minimum redundancy codes [J]. Proc IRE (IEEE) 40(9):1098–1101
10. Ilday FÖ, Buckley JR, Clark WG et al (2004) Self-similar evolution of parabolic pulses in a laser [J]. Phys Rev Lett 92(21):213902
11. Jacquin AE (1992) Image coding based on a fractal theory of iterated contractive image transformations. IEEE Trans Image Process 1(1):18–30
12. Kim CS, Kim RC, Lee SU (1998) Fractal coding of video sequence using circular prediction mapping and noncontractive interframe mapping [J]. Image Process IEEE Trans 7(4):601–605
13. Kim IK, Park RH (1996) Still image coding based on vector quantization and fractal approximation [J]. Image Process IEEE Trans 15(4):587–597
14. Lai CM, Lam KM, Siu WC (2003) A fast fractal image coding based on kick-out and zero contrast conditions [J]. Image Process IEEE Trans 12(11):1398–1403
15. Li J, Chen G, Chi Z (2002) A fuzzy image metric with application to fractal coding [J]. Image Process IEEE Trans 11(6):636–643
16. Liu S, Cheng X, Lan C et al (2013) Fractal property of generalized M-set with rational number exponent [J]. Appl Math Comput 220:668–675
17. Liu S, Fu W, Deng H et al (2013) Distributional fractal creating algorithm in parallel environment [J]. Int J Distrib Sensor Netw. doi:10.1155/2013/281707
18. Liu S, Fu W, Zhao W et al (2013) A novel fusion method by static and moving facial capture [J]. Math Probl Eng. doi:10.1155/2013/503924
19. Liu M, Liu S, Fu W, et al. (2014) Distributional escape time algorithm based on generalized fractal sets in cloud environment [J]. Chinese Journal of Electronics
20. Lu J, Ye Z, Zou Y (2013) Huber fractal image coding based on a fitting plane [J]. Image Process IEEE Trans 22(1):134–145
21. Mandelbrot BB (1982) The fractal geometry of nature [M]. Freeman W H, San Francisco
22. Monro DM, Dudbridge F (1992) Fractal block coding of images [J]. Electron Lett 28(11):1053–1055
23. Press WH, Schechter P (1974) Formation of galaxies and clusters of galaxies by self-similar gravitational condensation [J]. Astrophys J 187:425–438
24. Rao KR, Yip P (1990) Discrete cosine transform: algorithms, advantages, applications [M]. Academic press, Boston
25. Shapiro JM (1993) Embedded image coding using zerotrees of wavelet coefficients [J]. Signal Process IEEE Trans 41(12):3445–3462
26. Smart DR (1980) Fixed point theorems [M]. CUP Archive
27. Turaga DS, Chen Y, Caviedes J (2004) No reference PSNR estimation for compressed pictures [J]. Signal Process Image Commun 19(2):173–184
28. Wang XY, Wang SG (2008) An improved no-search fractal image coding method based on a modified gray-level transform [J]. Comput Graph 32(4):445–450
29. Wang XY, Wang YX, Yun JJ (2010) An improved no-search fractal image coding method based on a fitting plane [J]. Image Vis Comput 28(8):1303–1308
30. Wang XY, Zhang DD (2014) Discrete wavelet transform-based simple range classification strategies for fractal image coding [J]. Nonlinear Dyn 75(3):439–448
31. Yang G, Liu S (2014) Distributed cooperative algorithm for set with negative integer by fractal symmetrical property. Int J Distrib Sensor Netw. doi:10.1155/2014/398583

32. Zhang Y, Wang X (2012) Fractal compression coding based on wavelet transform with diamond search [J]. Nonlinear Anal Real World Appl 13(1):106–112

Associate Professor Shuai Liu master's supervisor, male, born in 1982, He interesting area contains applied mathematics and complex computation. Following are his main 5 papers. [1] Liu S, Cheng X, LAN C, et al. Fractal property of generalized M-set with rational number exponent, Applied Mathematics and Computation, 2013, 220, 668-675, SCI (IF=1.6). [2] S Liu, W Fu, H Deng, et al. Distributional Fractal Creating Algorithm in Parallel Environment, International Journal of Distributed Sensor Networks, 2013 doi:10.1155/2013/281707, SCI (IF=0.8). [3] S Liu, W Fu, W Zhao. A Novel Fusion Method by Static and Moving Facial Capture, Mathematical Problems in Engineering, 2013. doi:10.1155/2013/503924, SCI(IF=1.1). [4] G Yang, S Liu. Distributed Cooperative Algorithm for k-M Set with Negative Integer k by Fractal Symmetrical Property, International Journal of Distributed Sensor Networks, 2014, doi: 10.1155/2014/ 398583, SCI (IF=0.8). [5] S Liu, X Cheng*, W Fu, et al. Numeric characteristics of generalized M-set with its asymptote [J]. Applied Mathematics and Computation, 2014, 243:767–774, SCI (IF=1.6).

Dr. Weina Fu female, born in 1982, Her interesting area contains moving recognition and multimedia encoding. Following are her main 5 papers. [1] W Fu*, Z Xu, S Liu, et al. The capture of moving object in video image, Journal of Multimedia, 6(6), 2011, 518-525, Ei. [2] S Liu*, W Fu, H Deng, et al. Distributional Fractal Creating Algorithm in Parallel Environment, International Journal of Distributed Sensor Networks, 2013 doi:10.1155/2013/281707, SCI (IF=0.8). [3] S Liu*, W Fu, W Zhao. A Novel Fusion Method by Static and Moving Facial Capture, Mathematical Problems in Engineering, 2013. doi:10.1155/2013/503924, SCI(IF=1.1). [4] S Liu, X Cheng*, W Fu, et al. Numeric characteristics of generalized M-set with its asymptote [J]. Applied Mathematics and Computation, 2014, 243:767–774, SCI (IF=1.6). [5] J Zhou, C Sun, W Fu, et al. Modeling, Design and Implementation of a Cloud Workflow Engine Based on Aneka, Journal of Applied Mathematics, 2014, Article ID 512476. SCI (IF=0.8)

Professor Liqiang He male, born in 1974, His interesting area contains image processing and pattern recognition. Following are his main 5 papers. [1] L HE*, G ZHANG, Y ZHANG. Speeding Up Best Neighborhood Matching Algorithm for High Definition Image on GPU Platform. International Journal of Image and Graphics. 2010, 11(3), 315-337, 2010, SCI. [2] *L. HE, G. ZHANG, J. JIANG. GPU Accelerated Parallel Branch Prediction For Multi/Many-Core Processor Simulation. International Journal of Numerical Analysis & Modeling, 2012, 9(2), 193-207, 2012, SCI. [3] G. Zhang, *L. He and Y. Zhang, Parallel Best Neighborhood Matching Algorithm Implementation on GPU Platform. In 1st International Workshop on Frontier of GPU Computing, conjunction with 10th IEEE International conference on Computer and Information Technology, pp.1140-1145, UK, June 29-July 1, 2010 (EI) [4] *L. He and Y. Zhang, A Rotate-based Best Neighborhood Matching Algorithm for High Definition Image Error Concealment. In International Symposium on Frontier of Computer Science, Engineering, and Applications (CSEA2010), pp.1393-1396, UK, June 29-July 1, 2010 (EI) [5] *L. He, Y. Sun and C. Zhang, Adaptive Subset Based Replacement Policy for High Performance Caching. In 1st JILP Workshop on Computer Architecture Competitions: Cache Replacement Championship, Held in conjunction with the 37th ISCA, Saint-Malo, France, June19-23,2010 (EI)

Prof. Jiantao Zhou doctoral supervisor, female, born in 1974, Her interesting area contains cloud computing and smart computing. Following are her main 5 papers. [1] JZhou, C Sun, W Fu, et al. Modeling, Design and Implementation of a Cloud Workflow Engine Based on Aneka, Journal of Applied Mathematics, 2014, Article ID 512476. SCI (IF=0.8) [2] J Zhou, J Liu, J Wu, et al. A Latent Implementation Error Detection Method for Software Validation. Journal of Applied Mathematics, Volume 2013, Article ID 138287, SCI (IF=0.8) [3] J Liu, X Ye, J Zhou. Test Purpose Oriented I/O Conformance Test Selection with Colored Petri Nets. Journal of Applied Mathematics, Volume 2014 (2014), Article ID 645235, SCI (IF=0.8). [4 J Zhao, J Zhou. Translation Rules and a Supporting Tool for Model-based Reuse. 2012 I.E. 36th International Conference on Computer Software and Applications Workshops (COMPSAC 2012), 310-315. [5] J Zhou, C Lan, N. William, et al. A Quantitative Characterization of Cross Coverage. IEEE Transaction on Computers, 2014, (in press)

Dr. Ming Ma male, born in 1981, His interesting area contains image processing and multimedia compression. Following are his main 5 papers. [1] M. Ma, H.- K Yun, I.-H Park Etc, Engineering-SaaS CAD System for Embedded System Design, FlowrianII, IP-SOC-2010 IP Based Electronics System Conference & Exhibition, Nov.30 - Dec.1, 2010, Grenoble, France [2] M. Ma, K. Singh, D. -W. Park, Syungog An, Use of Region-Oriented Segmentation in Coin Recog nition, Key Engineering Materials Vols. 277-279, 2005, pp. 375-382, Trans Tech Publications, Switz erland. [3] M. Ma, K. Singh, D. -W. Park, Syungog An, Image Retrieval By Contents / Using Color & Edge, The Journal of Korean Association of Computer Education Vol.8 No.1, January, 2005 [4] M. Ma, D. -W. Park, Integrating Color, Texture and Edge Features for Content-Based Image Retrieval, Koran Journal of the Science of Emotion & Sensibility Vol.7 No.4, December 2004 [5] M. Ma, G. -J. Liu, K. Singh, D. -W. Park, Use of Region-Oriented Segmentation in Coin Recogniti on, Proc. of International Women's Conference on BIEN-Technology, Daejeon, South Korea. November , 2003